Robotic Slicing of Fruits and Vegetables: Modeling the Effects of Fracture Toughness and Knife Geometry

Prajjwal Jamdagni and Yan-Bin Jia

***Abstract*— Slicing is an important skill for a robot to learn as it is more efficient and results in less deformation in comparison with cutting by pressing. Cutting experiments with foods have indicated that the ease of slicing is caused by a decrease in fracture toughness. In this paper, we formally characterize this decrease based on the work needed to maintain the critical strain for fracture. Forces generating fracture and deformation and overcoming friction are predicted using the finite element method (FEM) and based on fracture mechanics. Extending our previous work [1] on cutting by pressing with a straight knife edge, we model general slicing and knife geometry (i.e., a curved edge). Experiments over potatoes and eggplants have demonstrated the accurate modeling of the overall cutting force during slicing, which could be leveraged for control of cutting by the robot to demonstrate human-level skills in the near future.**

I. Introduction

In the food industry, there exists a great demand for workers who can prepare fruits and vegetables for cooking purpose. This is a tedious job with repetitive actions and long working hours, and thus has a large workforce turnover. In addition, the COVID-19 pandemic is placing an increasing demand for health, hygiene, and safety during food preparation. These can be effectively addressed by employing robots which can work tirelessly at this job in a safe and hygienic manner. Skills such as chopping and slicing will be essential for such robots.

Experience tells us that slicing an object with a kitchen knife is a lot easier than pressing with it. Robots need to take advantage of the efficiency of the slicing action. In our previous work [1], a model was presented for cutting by (vertically downward) pressing with a straight knife edge based on fracture mechanics and the finite element method (FEM). The object was divided into several cross sections so cutting could be modeled as crack propagation independently within these 2-dimensional (2D) slices. This work, however, did not model more skillful moves such as slicing or the effect of knife geometry.

Atkins *et al.* [2] presented an energy-based analytical model of slicing under two assumptions. First, the cutting force and the knife displacement were coincident in the plane of cutting. This assumption does not appear to be true for cutting of deformable objects. The reason behind is that there exist different sources of origin for tangential and normal forces on the knife. While the normal force results from a normal compression, the tangential force results from shearing due to the friction between the knife edge and the object. We adopt generalized plane strain assumption to decouple the two forces [3], [4] and use the FEM for calculation. The second assumption by Atkins *et al.* was that the fracture toughness of an object during slicing would always be the same as during pressing. Again, this is not true, as we have found in our experiments that the fracture toughness changes during slicing. Less deformation is required during slicing to reach the critical maximum principal strain for fracture [5], which in turn results in a decrease in the fracture toughness. In this paper, we characterize such decrease during slicing by examining the strain below the knife edge.

Our previous work [1] used a fixed set of cross sections, an approach no longer suitable for cutting with a curved knife edge. This is because a set of cross sections normal to the knife edge at one time instant will no longer be normal at the next instant as the edge slices through the object. In this paper, we tackle this issue by continuously updating the cross sections based on the knife trajectory and current crack front which consists of points inside the object in contact with the knife edge.

This paper focuses on modeling of slicing by a curved knife attached to a robotic arm. Section II discusses related works from fracture mechanics and soft tissue cutting. In Section III, the change in fracture toughness during slicing with a straight knife edge is characterized based on the maximum principal strain below the edge. In Section IV, slicing with a curved knife edge is modeled. Experimental results are presented in Section V. Section VI concludes with some directions for future research.

A vector is represented by a lowercase letter in bold, e.g., $\boldsymbol{p} = (p_x, p_y)^T$, with its x- and y-coordinates denoted by the same (non-bold) letter with subscripts x and y, respectively.

II. Related Work

Soft tissue cutting is traditionally modeled as crack propagation based on fracture mechanics. Estimation of fracture toughness was done for ductile materials [6], and during the insertion of a needle into soft issue aided by FEM-based simulation [7]–[9]. FEM methods, both linear [10] and nonlinear [11], were used in surgical simulation of soft tissue cutting, with a comprehensive survey conducted in [12].

*Support for this research has been provided by the US National Science Foundation under Grant IIS-1651792. Any opinions, findings, and conclusions or recommendations expressed in this material are those of the authors and do not necessarily reflect the views of the National Science Foundation.

*We would like to thank Xiaoqian Mu and Yuechuan Xue for their early help with experiments. We also thank anonymous reviewers for their valuable feedback.

The authors are affiliated with the Department of Computer Science, Iowa State University, Ames, IA 50011, USA. prajjwal, jia@iastate.edu.

A model for compression cutting of bio-materials, and the effect of blade sharpness were presented [13]. Stress distribution and its effect on the fracture force during slicing were also investigated [14], [15]. An energy-based model explained the reduction in fracture force due to slicing under the assumption of constant fracture toughness [2]. This model was used to predict the force and torque generated from slicing thin flexible materials with negligible deformations [16]. Reduction in frictional force during soft material cutting was found to be related to a large inclination angle of the blade [17]. In paper industry, fracture mechanics is applied to model crack propagation during the slicing of a paper stack and the effect of friction on facilitating the process [18], [19].

Ease of slicing was attributed to the change from a global deformation during compression to a local shear deformation [5]. For soft tissues, slicing made it easier to achieve the critical stress or strain for fracture [20]. The aforementioned works all pointed at varying fracture toughness with slicing angle.

Investigations were conducted on strategies for robotic cutting based on adaptive control using position and velocity history [21] and impedance control for force tracking [22]. Soft material cutting has employed force/vision based control strategies for trajectory following and object stabilization [23], [24]. In [25] a three-phase cutting strategy was introduced to combine position, force, and impedance controls.

III. Slicing With A Straight Knife Edge

In [1], we modeled the cutting of a deformable object when the knife edge is straight, horizontal (parallel to the z-axis as shown in Fig. 1), and translating downward in the vertical yz-plane, which coincides with the blade's plane of symmetry. Assuming plane strain at the contact between the knife edge and the object, we divided the object by multiple cross sections parallel to the xy-plane. Cutting of each cross section was modeled using linear elastic fracture mechanics:

$$dW = dW_c + dW_f = R_c\, ds + dU + dW_f, \qquad (1)$$

where dW, dW_c, dW_f are the total work, the work done to propagate crack, and the work done to overcome friction by the knife for an infinitesimal movement dy, R_c is the *fracture toughness*, defined as the energy required to increase the crack by unit area, ds is the increment in crack length, and dU is the change in strain energy. It should be noted that since we are cutting a 2D cross section, force has the unit N/m, and work and energy have the unit N. Strictly speaking, U and W_f are both functions of s that have no closed forms in general. We simplified (1) by neglecting friction while calculating ds. We used the *energy release rate*, $R = (dW_c - dU)/ds$, to check if the crack length increases at least by a fixed small amount $ds = \delta$, *i.e.*, if $R \geq R_c$. After confirming that the crack propagates, we determined the actual value of ds by using the bisection method such that $R = R_c$. Once ds was determined, dW_f was calculated using normal force on the side of the knife and ds as the relative displacement. FEM was used to calculate the strain energy and the force over a given mesh of the cross section. We integrated over all the cross sections to predict the total force by the knife edge. This work is referred to as cutting by *pressing*, where the knife's velocity is normal to the knife edge.

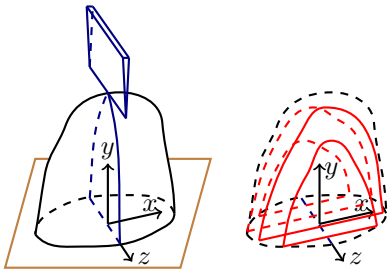

Fig. 1: Object represented by evenly spaced cross sections parallel to the xy-plane.

In contrast, cutting by *slicing* refers to cutting when the knife's velocity also has a component along its (straight) edge, that is, in the z-direction. This makes it easier to reach critical stress or strain for fracture at the contact [5]. The critical maximum principal strain has been found to maintain a relatively constant value for different ratios between normal and tangential force [20], [26]. Hence this strain is used to characterize the change in fracture toughness during slicing. The plane strain assumption used in our previous work [1] is replaced with the following generalized version to take tangential force into account:

(A1) All planes normal to the knife edge undergo the same deformation.

We also make a second assumption:

(A2) Deformation in the knife's cutting plane, the yz-plane, only happens in its velocity direction.

We will only consider translations of the knife in this paper.

A. Strain Below the Knife Edge

To obtain the strain at a point $\boldsymbol{p}$ right below the knife edge within a cross section, we model the object as a half-space and the contact between the knife edge and the object is a narrow infinite strip along the knife edge, as shown in Fig. 2. A local coordinate frame $x'y'z'$ is defined, such that the knife edge stretches along the x'-axis, and the z'-axis passes through the point $\boldsymbol{p}$ at which we want to characterize the strain. The angles θ_1 and θ_2 are between the z'-axis and the lines joining $\boldsymbol{p}$ with the endpoints of the segment where the edge strip intersects with the $y'z'$-plane. Let σ_{ii} be the normal stress, where i is the direction of the normal stress, and σ_{ij} be the shear stress, where i is the direction of the normal to the plane in which the shear stress is applied and j is the direction of the shear stress. We also define two directions, $\hat{\boldsymbol{n}}$, normal to the knife edge and coincident with the z'-axis, and $\hat{\boldsymbol{t}}$, tangential to the knife edge and coincident with x'-axis. Let f_n and f_t be the normal and tangential forces per unit surface area, respectively, applied by the knife edge on the object.

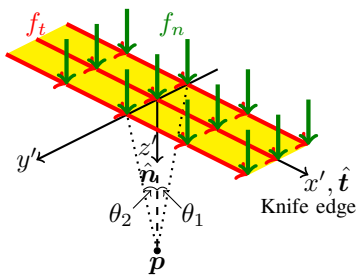

Fig. 2: Stress at a point due to normal and tangential strip loading.

Boussinesq's [27] solution for the stress at any point in an infinite half-space due to a normal point load on its boundary plane is integrated over the contact area between the knife edge and the object to calculate the stress due to a normal strip loading f_n at $\boldsymbol{p}$:

$$\begin{aligned}
\sigma_{z'z'} &= \big(\theta_2 - \theta_1 + \big(\sin(2\theta_2) - \sin(2\theta_1)\big)/2\big)\, f_n/\pi,\\
\sigma_{y'y'} &= \big(\theta_2 - \theta_1 - \big(\sin(2\theta_2) - \sin(2\theta_1)\big)/2\big)\, f_n/\pi,\\
\sigma_{x'x'} &= \nu(\sigma_{y'y'} + \sigma_{z'z'}),\\
\sigma_{y'z'} &= \sigma_{z'y'} = \big(\sin^2\theta_2 - \sin^2\theta_1\big)\, f_n/\pi,\\
\sigma_{x'y'} &= \sigma_{y'x'} = \sigma_{z'x'} = \sigma_{x'z'} = 0,
\end{aligned} \tag{2}$$

where ν is the Poisson's ratio. Similarly, Cerruti's [28] solution for the stress at any point in an infinite half-space due to a tangential point load f_t at the surface is integrated over the contact area between the knife edge and the object to obtain stress at $\boldsymbol{p}$ due to a tangential strip load:

$$\begin{aligned}
\sigma_{x'z'} &= \sigma_{z'x'} = (\theta_2 - \theta_1)\, f_t/\pi,\\
\sigma_{x'y'} &= \sigma_{y'x'} = (\ln|\cos\theta_1| - \ln|\cos\theta_2|)\, f_t/\pi,\\
\sigma_{x'x'} &= \sigma_{y'y'} = \sigma_{y'z'} = \sigma_{z'z'} = 0.
\end{aligned} \tag{3}$$

For a point just below the knife edge, $\theta_1 = -\pi/2$ and $\theta_2 = \pi/2$. Substituting these values into (2) and (3), we obtain

$$\begin{aligned}
&\sigma_{x'x'} = 2\nu f_n, \quad \sigma_{y'y'} = f_n, \quad \sigma_{z'z'} = f_n,\\
&\sigma_{x'y'} = 0, \qquad \sigma_{y'z'} = 0, \qquad \sigma_{z'x'} = f_t.
\end{aligned}$$

Using Hooke's law, the strain tensor can be calculated as

$$\boldsymbol{\epsilon} = \frac{1}{E}\begin{pmatrix} 0 & 0 & f_t(1+\nu)\\ 0 & f_n(1-\nu-2\nu^2) & 0\\ f_t(1+\nu) & 0 & f_n(1-\nu-2\nu^2)\end{pmatrix},$$

where E is the Young's modulus. The largest eigenvalue of this strain tensor gives us the maximum principal strain:

$$\begin{aligned}
\epsilon_{\max} = (f_n/2E)\Big((1-\nu-2\nu^2)\\
+\sqrt{(1-\nu-2\nu^2)^2 + 4\big((f_t/f_n)(1+\nu)\big)^2}\Big).
\end{aligned} \tag{4}$$

B. Varying Fracture Toughness With the Slice-Push Ratio

Atkins *et al.* [2] introduced the slice-push ratio ξ as the ratio between the knife's tangential displacement dt and normal displacement dn. They also assumed that it is equal to the ratio between the knife's tangential force F_t and normal force F_n, that is, $\xi = dt/dn = F_t/F_n$. But this is not the case when the object is deformable. The tangential force is a shear force, and therefore proportional to the shear modulus G and the tangential displacement. On the other hand, the normal force is a compression force that is proportional to the Young's modulus E and the normal displacement. We propose the following new form of their ratio:

$$\frac{F_t}{F_n} = \frac{f_t}{f_n} = \frac{G}{E}\frac{dt}{dn} = \frac{1}{2(1+\nu)}\xi.$$

Substituting the ratio into (4), the maximum principal strain for pressing ($\xi = 0$) and slicing ($\xi \neq 0$) are derived as

$$\epsilon^p_{\max} = (f^p_n/E)(1-\nu-2\nu^2), \text{ and}$$
$$\epsilon^s_{\max} = (f^s_n/2E)\big((1-\nu-2\nu^2) + \sqrt{(1-\nu-2\nu^2)^2 + \xi^2}\big),$$

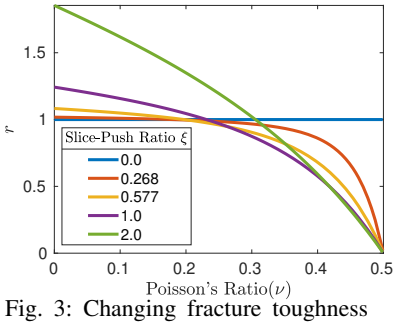

Fig. 3: Changing fracture toughness during slicing as measured by its ratio to the constant value during pressing.

respectively. As the critical maximum principal strain for fracture onset remains fixed [20], [26], we calculate the ratio between the normal forces during slicing and pressing for the same maximum principal strain as

$$f^s_n/f^p_n = 2/(1 + \sqrt{1 + \big(\xi/(1-\nu-2\nu^2)\big)^2}).$$

During the continuous cutting of an infinite half-space, the change in strain energy is negligible. Assuming no friction at the knife's sides, all the work done by the knife gets converted into extending the crack. As the state of critical maximum principal strain is constantly maintained at the knife edge, for the same vertical displacement dn, the ratio between the fracture toughness R^s_c for slicing and the fracture toughness R_c for pressing can be derived as

$$\begin{aligned}
r = \frac{R^s_c}{R_c} &= \frac{(f^s_n dn + f^s_t dt)/dn}{(f^p_n dn)/dn} = \frac{f^s_n}{f^p_n}\left(1 + \frac{\xi^2}{2(1+\nu)}\right)\\
&= \frac{2}{1 + \sqrt{1 + \big(\xi/(1-\nu-2\nu^2)\big)^2}}\left(1 + \frac{\xi^2}{2(1+\nu)}\right).
\end{aligned}$$

Fig. 3 plots the value of r relative to Poisson's ratio for different ξ values.

C. Slicing a Cross section

The slicing of a cross section is modeled in an iterative manner, as in our previous work [1]. Within one iteration, the knife will move downward until the energy release rate $R = (dW_c - dU)/ds$ exceeds the fracture toughness R^s_c for a very small, fixed increase in crack length $ds = \delta$. dW_c has a vertical component $dW_n = F_n\, dn$ and a horizontal component $dW_t = F_t\, dt$. We use the generalized plane strain condition [4] to decouple the two forces F_n and F_t. Just like F_n and dW_n were calculated using the FEM in [1], F_t and dW_t can also be determined using the FEM here as the antiplane shear component of generalized plane strain [4] by solving the Laplace equation, $\nabla^2 u_t = 0$, where u_t is the displacement in the tangential direction. Two boundary conditions are imposed. The bottom of the cross section is fixed, so are the nodes in contact with the knife edge. The FEM is used for calculating dU. To determine the actual value of ds, we increase δ in integer multiples until locating an interval that bounds the maximum crack length. Then we use bisection to calculate ds such that $R = R^s_c$. Then the friction work, dW_f, is calculated using the normal force on both sides of the blade (obtained from FEM simulation), friction coefficient, and a relative displacement in the knife velocity direction with ds as its vertical component. This is repeated for each cross section and integrated over all cross sections to get the total force exerted and work done by the knife as in [1].

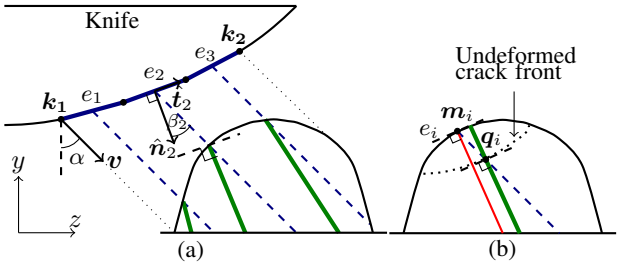

Fig. 4: (a) Approximating the curved edge with piecewise linear segments e_i. Dashed blue lines represent the trajectories of the segments' midpoints. Solid green lines show the side view of the initial cross sections associated with each segment. (b) Replacing old cross section (red) associated with the segment e_i. The new cross section (green) passes through the intersection of the crack front (dotted) and the midpoint $\boldsymbol{m}_i$'s trajectory (dashed blue), and lies in a plane normal to the segment e_i in the undeformed state.

IV. Slicing With A Curved Knife Edge

Until now, we have modeled slicing with a translating straight knife edge. The object is divided into cross sections normal to the knife edge in its undeformed state. Choosing cross sections that are not normal to the edge may lead to incorrect calculation of stress tensor at their contact points with the knife edge. These cross sections slide over the knife edge during slicing. Along a curved knife edge, the directions of the tangent and normal vary, and we need to generate new cross sections as the knife moves, which is a costly process due to meshing. To reduce the number of times of such generations, a piecewise linear approximation of the edge is used. See Fig. 4(a). Under assumption (A2), we find the endpoints $\boldsymbol{k_1}$ and $\boldsymbol{k_2}$ of the arc on the knife edge that will come in contact with the object, as shown in Fig. 4(a). The arc is divided into m equal curve segments by length. The ith segment is approximated by a linear segment e_i which connects its end points, with a unique normal $\hat{\boldsymbol{n}}_i$ and tangent $\hat{\boldsymbol{t}}_i$. The segment's slice-push ratio is $\xi_i = \tan\beta_i$, where β_i is the angle between $\hat{\boldsymbol{n}}_i$ and the knife velocity $\boldsymbol{v}$. Its movement is tracked by its midpoint's trajectory (shown as a dashed blue line). Initially, the cross section associated with the segment is normal to it, and passes through its midpoint's first point of contact with the object (shown as a green line in side view).

To generate a cross section for the segment e_i at the time instant, we must find a point $\boldsymbol{q}_i$ on the object that coincides with the segment's midpoint $\boldsymbol{m}_i$. See Fig. 4(b). Under assumption (A2), $\boldsymbol{m}_i$ will only come in contact with those points inside the object that are on its trajectory. In addition, $\boldsymbol{q}_i$ must lie on the crack front. Also, the new cross section should be normal to the segment in the undeformed state. These conditions determine a unique cross section for the segment shown as the green line in Fig. 4(b). The crack front is represented by a second degree polynomial fit over all the points $\boldsymbol{q}_i$, $1 \leq i \leq m$.

V. Experiments

Three experiments were conducted. The first one was to validate our model for varying fracture toughness during slicing. A straight edge knife was used to slice cuboid pieces around the core of a single object to reduce the influences by geometry and mechanical properties. The second experiment was to validate our model for cutting with a curved knife edge, again using cuboid pieces. The last experiment was done with objects in their natural shapes to measure modeling accuracy in practical cutting situations. Cutting was carried out by rigidly attaching a kitchen knife to an ADEPT Cobra 800 robot, as shown in Fig. 5. Force and torque data were recorded by a 6-axis F/T sensor (Delta IP65) from ATI Industrial Automation, which was mounted between the knife and the robot's open end. The speed of knife translation was fixed at 0.00625m/s. Table I lists the quartic polynomials representing the knife edge and spine. Each experiment was performed on two objects: a potato (hard and homogeneous) and an eggplant (soft and non-homogeneous). Table II lists their physical parameters. Initial values for Young's modulus (E) and Poisson's ratio (ν) were taken from [29] and [30] and then tuned over several cutting trials using the initial slope of force-displacement curve before fracture initiates. The same parameter values were used for the first two experiments where cuboid pieces (prepared from a single potato/eggplant, and illustrated in Fig. 6(a)) were cut. A different set of parameter values was used when we cut the whole objects with their skins intact. Also, as an eggplant is soft and has a very tough skin, we set a larger initial fracture toughness and then used a smaller value after fracture due to stress concentration at the crack tip for soft materials.

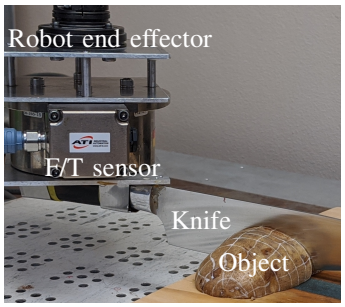

Fig. 5: Experimental setup.

A. Slicing With a Straight Knife Edge

Cutting was first carried out using a segment of the knife edge close to the handle. Four cuboid pieces from a potato were used, as shown in Fig. 6(a). Each piece was sliced

TABLE I: Knife geometry.

knife tip(m)	$x = 0,\ y = 0.034,\ z = 0.19$
knife edge(m)	$y = 83.4z^4 - 22.05z^3 + 2.48z^2 - 0.06z$
knife spine(m)	$y = -33.06z^4 + 6.9z^3 - 0.4z^2 + 0.005z + 0.04$

TABLE II: Mechanical properties of the objects in the experiments: Young's modulus (E), Poisson's ratio (ν), coefficient of blade-material friction (μ), interior fracture toughness (R_c), and initial fracture toughness ($R_c^{'}$).

Object	E (N/m^2)	ν	μ	R_c (N/m)	$R_c^{'}$ (N/m)
Experiments with cuboid pieces (without skin)					
Potato	2×10^6	0.4	0.1	150	150
Eggplant	0.4×10^6	0.35	1.0	140	275
Experiments with whole objects (with skin)					
Potato	2×10^6	0.4	0.1	230	230
Eggplant	0.55×10^6	0.35	1.0	260	650

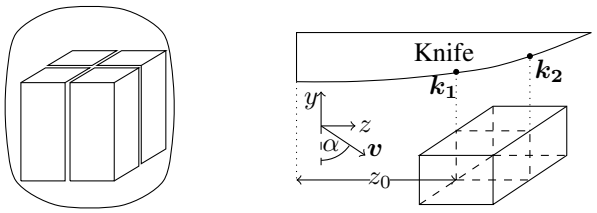

(a) (b)

Fig. 6: (a) Piece preparation. (b) Cutting setup: α is the angle between the velocity $\boldsymbol{v}$ and the y-axis, and z_0 is the horizontal distance of the piece from one endpoint of the knife edge.

with a different slice-push ratio, $\xi = \tan\alpha$, where α is the angle between the velocity direction and the y-axis, as shown in Fig. 6(b). Fig. 7(a) plots the sensed force per unit length in the vertical y-direction and horizontal z-direction, and the total work per unit length against the vertical knife displacement. Force and work for each piece were divided by its length along the z-axis for comparison. Smoothness of the work plot is due to integration of the knife force over the knife displacements. The force plots are instantaneous sensor readings. Simulation was done for each piece by slicing one (uniform) 2D cross section using our model, as shown in Fig. 7(b). Figs. 7(c) and (d) respectively show the plots for the experiment and simulation repeated for an eggplant.

The first experiment indicates that force and velocity are not coincident during the cutting of deformable objects. For instance, in Fig. 7(a) the horizontal to vertical force ratio does not match the slice-push ratio (ξ) used for the experiment. Also, the fracture toughness did not remain constant. As shown in the last column, the total work per unit length done by the knife decreased as ξ increased. However, for a very large ξ value, the total work increased for potato. This can be explained by the fact that the decrease in the fracture toughness during slicing saturated at higher ξ values (see Fig. 3), and the work done to overcome friction increased with the total displacement. The total work for the eggplant shows a considerable decrease for the same case because it is very anisotropic with fibers running along its axis, and the mechanism for fracture under shear may be very different for compression. This is evident in Fig. 7(c) from the fact that, while the horizontal force increased with ξ, it suddenly dropped at a very high ξ value. In Fig. 7(c), the horizontal force at α = 0° had a large negative value when fracture started after a large deformation. This could be due to unequal fracture across the knife edge. In Fig. 7(d), a jump in work was observed for eggplant due to friction work as a large crack was happening after a large deformation.

B. Pressing With a Curved Knife Edge

Four new cuboid pieces were prepared as before. Cutting was carried out using different sections of the knife by varying the horizontal distance z_0 of each piece to the left endpoint of the knife edge (where it connects the knife's handle). See Fig. 6(b). The knife moved only vertically downward ($\alpha = 0$). For simulation, the knife edge's cutting section (between $\boldsymbol{k_1}$ and $\boldsymbol{k_2}$ in the figure) is discretized into ten segments. A 3D cuboid mesh is created for each piece

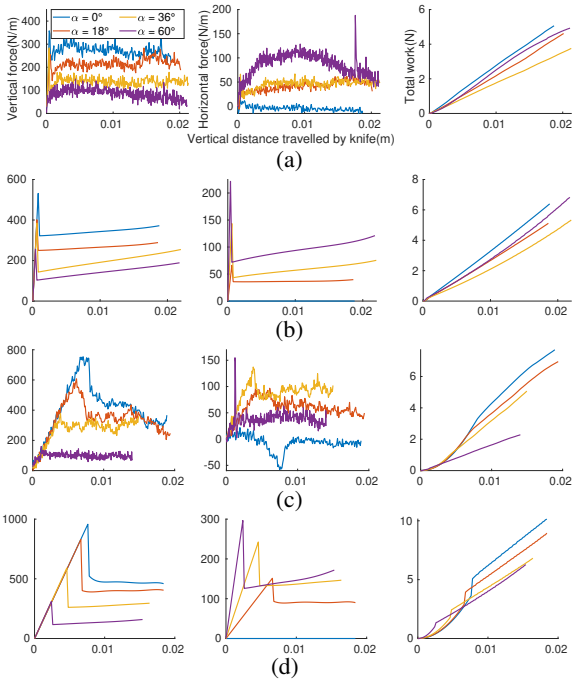

Fig. 7: Experiment and simulation results for straight knife edge slicing of cuboid objects with angle between the velocity direction and the y-axis $\alpha = \{0°, 18°, 36°, 60°\}$. The vertical force ($y$-direction), the horizontal force (z-direction) and the total work, plotted in the three columns, respectively, are divided by the length of the cuboid along the z-direction (see Fig. 6(b)). (a) Experiment on a potato cuboid. (b) Simulation for the experiment (with column correspondence). (c) Experiment on an eggplant. (d) Its simulation. In every plot the horizontal axis is knife displacement in the downward y-direction.

for generating cross sections, which are updated as described in Section IV for each step of knife displacement by 1 mm. The experiment and our simulation results are presented in Figs. 8 and 9 for potato and eggplant, respectively.

As illustrated in Fig. 6(b), the knife edge curves more as z_0 increases, resulting in a longer duration to establish contact with the object. For a potato, fracture happened very early on. Fig. 8 shows that the slopes of force and work decreased in the meantime, before they were stabilized at the maximum contact by the knife edge. Fig. 9 shows that fracture of an eggplant happened very late, with the effect of increasing z_0 value reflected in the initial slopes of the vertical force plots. For cases with very small horizontal force, sensed values were not accurate, especially in the case of cutting a potato.

C. Slicing Natural Shapes With a Curved Knife Edge

Three half-potatoes were prepared beforehand with a flat base to stabilize them on the cutting board (see Fig. 5). The experiments were conducted by varying z_0 and α for each piece. For simulation, every piece was laser scanned to generate a 3D mesh. Figs. 10 and 11 show the experiment and simulation results for potato and eggplant, respectively.

Our model predicts the forces and work reasonably well considering three different potatoes (eggplants) were cut. Tough skin on the eggplant decreases the horizontal force prediction accuracy as our generalized plane strain assumption may no longer be valid.

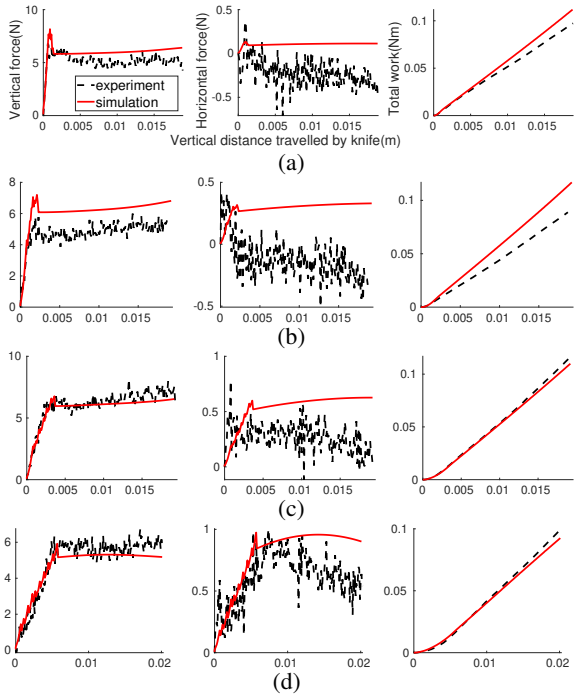

Fig. 8: Vertical and horizontal forces, and total works from cutting four cuboid potato pieces generated by a curved knife edge translating vertically downward (cf. Fig. 6(b)). Cutting was performed using different sections of the knife edge with z_0 values: (a) 0.02 m, (b) 0.0765 m, (c) 0.1135 m, and (d) 0.14 m. The horizontal axis is knife displacement in the downward y-direction. In each diagram, black dots represent the experimental result and the red curve represents the simulation result.

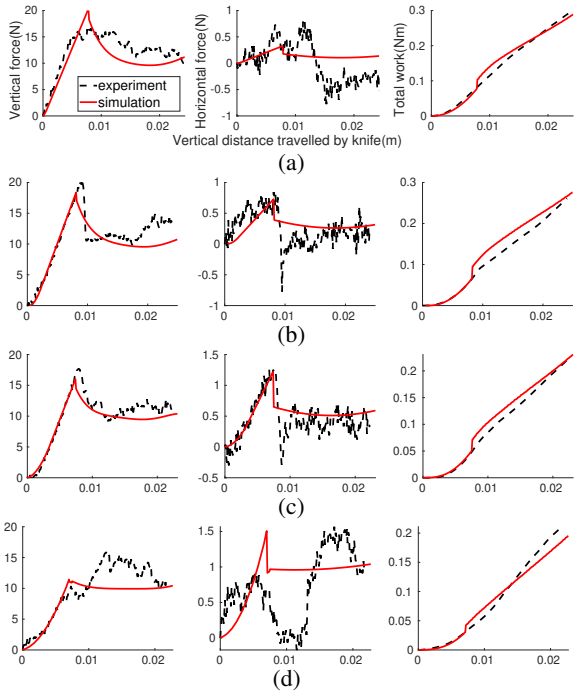

Fig. 9: Experiment and simulation results for cutting cuboid eggplant pieces by a curved knife edge moving vertically downward. Same sequence of four values of z_0 as given in Fig. 8 were used.

VI. Discussion

We have proposed a model for characterizing the change in fracture toughness during slicing based on critical maximum principal strain. This model can be combined with our previous work to accurately predict the forces during cutting by slicing. In addition, we have also proposed a method to model the effect of knife geometry by dynamically updating cross sections according to the knife trajectory and crack front position during cutting. The fracture and friction force predicted by the model can be used to separate the contact force due to the cutting board from sensor readings for control purposes, and the predicted total work can be used for efficient motion planning.

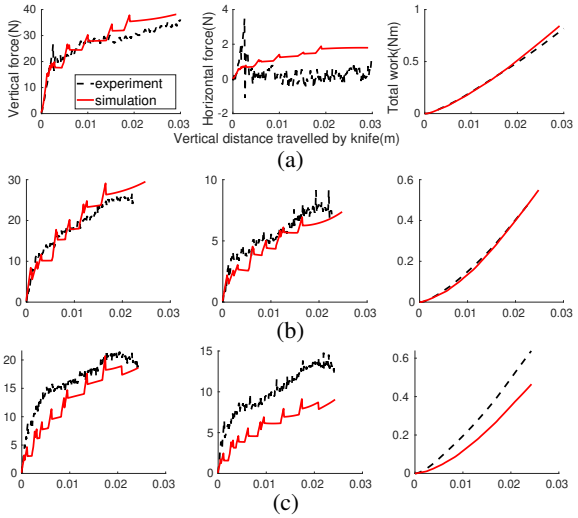

Fig. 10: Experiment and simulation results for cutting general shaped potatoes by a curved knife edge, where (α, z_0) takes on the values: (a) (0°, 0.046m) (b) (24°, 0.087m), and (c) (45°, 0.139m).

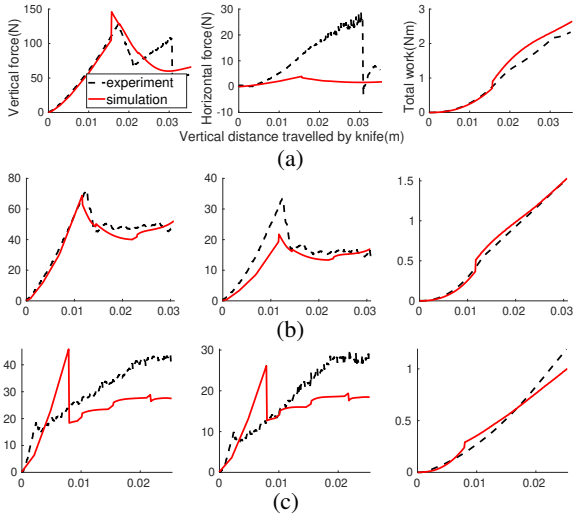

Fig. 11: Experiment and simulation results for cutting general shaped eggplants by a curved knife edge. Same three pairs of values of (α, z_0) as in Fig. 10 were used sequentially.

Our current model is limited by varying mechanical properties of the foods which depend on several factors such as time of storage, temperature, humidity etc. In the future, we would like to do an online estimation for them based on the history of cutting. Effects of tough skin on the fruits and vegetables as well as anisotropic structures like fibers also need to be explored in depth. Further investigation on the role played by friction during slicing is needed. We would also like to explore our model's application in knife control to achieve smooth cutting of non-homogeneous objects.

REFERENCES

[1] P. Jamdagni, and Y.-B. Jia. "Robotic cutting of solids based on fracture mechanics and FEM," in *Proc. IEEE/RSJ Int. Conf. Intell. Robots Syst.*, 2019, pp. 8246–8251.

[2] A. G. Atkins, X. Xu, and G. Jeronimidis. "Cutting, by 'pressing and slicing,' of thin floppy slices of materials illustrated by experiments on cheddar cheese and salami," *J. Materials Sci.*, vol. 39, pp. 2761–2766, 2004.

[3] T. L. Anderson. *Fracture Mechanics: Fundamentals and Applications*. CRC Press, Boca Raton, Fl 33487-2742, US, 2005.

[4] A. H.-D. Cheng, J. J. Rencis, and Y. Abousleiman. "Generalized plane strain elasticity problems," *Trans. Model. Simul.*, vol. 10, pp. 167–174, 1995.

[5] E. Reyssat, T. Tallinen, M. Le Merrer, and L. Mahadevan. "Slicing softly with shear," in *Phys. Rev. Lett.*, vol. 109, pp. 244301-1–244301-5, 2012.

[6] A. G. Atkins. "Toughness and cutting: a new way of simultaneously determining ductile fracture toughness and strength," *Engr. Fracture Mechanics*, vol. 72, pp. 850–860, 2004.

[7] M. Khadem, C. Rossa, R. S. Sloboda, N. Usmani, and M. Tavakoli. "Mechanics of tissue cutting during needle insertion in biological tissue," *IEEE Robot. Autom. Letters*, vol. 1, no. 2, pp. 800–807, 2016.

[8] C. Gokgol, C. Basdogan, and D. Canadinc. "Estimation of fracture toughness of liver tissue: Experiments and validation," *Medical Engr. Phy.*, vol. 34, pp. 882–891, 2012.

[9] T. Azar and V. Hayward. "Estimation of the fracture toughness of soft tissue from needle insertion," in *LNCS*, Springer-Verlag Berlin, 2008, pp. 166–175.

[10] T. Chanthasopeephan, J. P. Desai, and A. C. W. Lau. "Modeling soft tissue deformation prior to cutting for surgical simulation: Finite analysis and study of cutting parameters," *IEEE Trans. Biomed. Engr.*, vol. 54, no. 3, pp. 349–359, 2007.

[11] B. Ghali and S. Sirouspour. "Nonlinear finite element-based modeling of soft tissue cutting," in *Proc. IEEE Toronto Int. Conf. Sci. Tech. Humanity*, 2009, pp. 141–146.

[12] B. Takabi, and B. L. Tai. "A review of cutting mechanics and modeling techniques for biological materials," *Medical Engr. Phys.*, 45:1–14, 2017.

[13] D. Zhou and G. McMurray. "Modeling of blade sharpness and compression cut of biomaterials," *Robotica*, vol. 28, pp. 311–319, 2010.

[14] D. Zhou, M. R. Claffee, K.-M. Lee, and G. V. McMurray. "Cutting, 'by pressing and slicing', applied to robotic cutting bio-materials, Part I: Modeling of stress distribution," in *Proc. IEEE/RSJ Int. Conf. Intell. Robots Syst.*, 2006, pp. 2896–2901.

[15] D. Zhou, M. R. Claffee, K.-M. Lee, and G. V. McMurray. "Cutting, 'by pressing and slicing', applied to robotic cutting bio-materials, Part II: Force during slicing and pressing cuts," in *Proc. IEEE/RSJ Int. Conf. Intell. Robots Syst.*, 2006, pp. 2256–2261.

[16] A. G. Atkins and X. Xu. "Slicing of soft flexible solids with industrial applications," *Int. J. Mech. Sci.*, vol. 47, pp. 479–492, 2005.

[17] A. Spagnoli, R. Brighenti, M. Terzano, and F. Artoni. "Cutting resistance of soft materials: Effects of blade inclination and friction," *Theo. Appl. Fracture Mechanics*, vol. 101, pp. 200–206, 2019.

[18] K.-R. Deibel, C. Raemy, and K. Wegener. "Modeling slice-push cutting forces of a sheet stack based on fracture mechanics," *Engr. Fracture Mechanics*, vol. 124–125, pp. 234–247, 2014.

[19] K.-R. Deibel, S. Lämmlein, and K. Wegener. "Model of slice-push cutting forces of stacked thin material," *J. Materials Processing Technology*, vol. 214, pp. 667–672, 2014.

[20] J. Wang, C. Li, and S.-C. Chen. "Sectioning soft materials with an oscillating blade," *Precision Engineering*, vol. 56, pp. 96–100, 2019.

[21] G. Zeng and A. Hemami. "An adaptive control strategy for robotic cutting," in *Proc. IEEE Int. Conf. Robot. Autom.*, 1997, pp. 22–27.

[22] S. Jung and T. C. Hsia. "Adaptive force tracking impedance control of robot for cutting nonhomogeneous workpiece," in *Proc. IEEE Int. Conf. Robot. Autom.*, 1999, pp. 1800–1805.

[23] P. Long, W. Khalil, and P. Martinet. "Modeling and control of a meat-cutting robotic cell," in *Proc. Int. Conf. Advanced Robot.*, 2013, pp. 61–66.

[24] P. Long, W. Khalil, and P. Martinet. "Force/vision control for robotic cutting of soft materials," in *Proc. IEEE/RSJ Int. Conf. Intell. Robots Syst.*, 2014, pp. 4716–4721.

[25] X. Mu, Y. Xue, and Y.-B. Jia. "Robotic cutting: Mechanics and control of knife motion," in *Proc. IEEE Int. Conf. Robot. Autom.*, 2019, pp. 3066–3072.

[26] N. Perez. *Fracture mechanics*. Kluwer Academic Publishers, 2004.

[27] J. Boussinesq. *Application des Potentiels a l'Etude de l'Euqilibre et du Mouvement des Solides Elastiques.* Gauthier-Villars, Paris, 1885.

[28] R. O. Davis, A. P. S. Selvadurai. *Elasticity and Geomechanics*. Cambridge University Press, New York, US, 1996.

[29] M. Bentini, C. Caprara, R. Martelli. "Physico-mechanical properties of potato tubers during cold storage," in *Biosystems Engineering*, vol. 104, pp. 25–32, 2009.

[30] S. M. Ashtiani, M. R. Golzarian, J. B. Motie, B. Emadi, N. N. Jamal, H. Mohammadinezhad. "Effect of loading position and storage duration on the textural properties of eggplant," in *Int. J. Food Properties*, vol. 19, pp. 814–825, 2016.